This article has been accepted for publication in a future issue of this journal, but has not been fully edited. Content may change prior to final publication. Citation information: DOI 10.1109/TMECH.2018.2873620, IEEE/ASME Transactions on Mechatronics

High-precision tracking control of a soft dielectric elastomer actuator with inverse viscoelastic hysteresis compensation

Jiang Zou and Guoying Gu

***Abstract*—In this paper, we present a new control approach for high-precision tracking control of a soft dielectric elastomer actuator (DEA) with inverse viscoelastic hysteresis compensation. To this end, we firstly investigate the viscoelastic response of the DEA and divide it into transition region and stable region. Then, the viscoelastic response is characterized by creep and hysteresis effects according to the different features of the two regions. Finally, a two-level tracking control approach is developed as: i) a direct inverse hysteresis compensation controller with a phenomenological hysteresis model is designed for the viscoelastic hysteresis description and compensation; and ii) a conventional proportional-integral feedback controller is combined to compensate for the model uncertainty and creep effect. To verify the effectiveness of the developed tracking control approach, several experiments are conducted with various reference sinusoidal trajectories. Experimental results show that: when the frequency of the trajectory is within the range of 0.1 Hz to 1 Hz, the maximum tracking error and the root-mean-square error decrease from 40.63% to 3.95% and 28.38% to 1.86%, respectively. This work is the first attempt to achieve high-precision tracking control of soft DEAs by combining a phenomenological-model feedforward compnesator and a feedback control law for the viscoelastic compensation, which may accelerate the practical applications of DEAs to soft robots.**

***Index Terms*—dielectric elastomer actuators, viscoelasticity, high-precision tracking control, direct inverse hysteresis compensation**

I. Introduction

DUE to the capability of large deformation and shape change, dielectric elastomer actuators (DEAs) show promising applications in the field of soft robotics [1]–[3]. In general, a DEA consists of an electro-active polymer membrane sandwiched by compliance electrodes [4]. When a high voltage is applied to the electrodes, the Maxwell stress squeezes the membrane, so that it will expand in area and decrease in thickness to keep a constant volume [5]. On the basis of this working principle, different DEAs have been invented, including rectilinear [6], [7], rotation [8], bending [9] and ballooning [10], [11] motions. During the past decade, there are diverse achievements on design of DEA driven soft robots, for instance, a soft fish [12] and a soft printable hexapod robot [13]. As one type of actuators, DEAs not only need to satisfy the functional movement of soft robots, but also acquire to achieve accurate positioning control for practical applications.

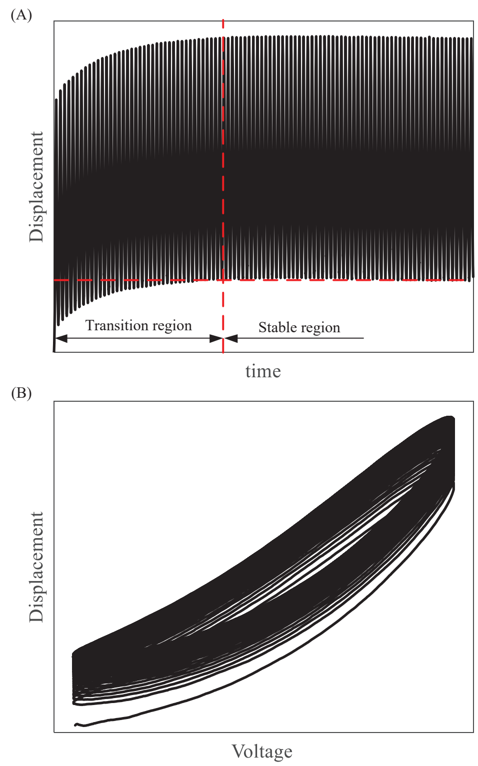

Fig. 1. Response of a dielectric elastomer actuator (DEA) under a sinusoidal voltage. (A) Creep effect; (B) Hysteresis effect.

However, high-precision tracking control of DEAs still remains challenging because of their inherent viscoelasticity. Based on the constitutive model of DEAs proposed in [14], the viscoelasticity can be generally explained by viscoelastic creep and hysteresis effects as shown in Fig. 1. The creep is a drift effect of the output displacement even though the exciting voltage keeps constant. In general, creep will dominant the response in the first few cycles and then become ignorable [14], [15]. It is known that the creep can be easily eliminated by a feedforward controller [15] or a conventional feedback controller (such as PID controller) [16]. In contrast, the hysteresis is non-smooth nonlinear between input voltage and output displacement over the whole response [14], [17].

This work was supported in part by the National Natural Science Foundation of China under Grant 51622506, in part by the Science and Technology Commission of Shanghai Municipality under Grant 16JC1401000. (Corresponding author: Guoying Gu).

J. Zou and G. Gu are with Soft Robotics and Biodesign Lab, Robotics Institute, School of Mechanical Engineering, Shanghai Jiao Tong University, and also with State Key Laboratory of Mechanical System and Vibration, Shanghai Jiao Tong University, Shanghai 200240, China. (e-mail: guguoying@sjtu.edu.cn; sj_ustb@sjtu.edu.cn).

This article has been accepted for publication in a future issue of this journal, but has not been fully edited. Content may change prior to final publication. Citation information: DOI 10.1109/TMECH.2018.2873620, IEEE/ASME Transactions on Mechatronics

In fact, it is also a great challenge to attain the high-precision performance of the systems with such kind of hysteresis, which leads, in the best case, to reduce the motion accuracy and, in the worst case, to destabilize the control system [17]–[19]. Therefore, in order to achieve high-precision tracking control of DEAs, the main challenge is owing to the viscoelastic hysteresis effect.

In previous literatures, some interesting works have been reported for control of DEAs, such as the PID control [20], [21], and self-sensing based close-loop control [22], [23]. However, they generally focus on compensating for the hyper-elasticity. Therefore, these control approaches are verified for tracking step trajectories, which may fail to track the period trajectories because the viscoelasticity is not taken into consideration. By taking the viscoelasticity into account, Seelecke $et.al.$ recently has proposed two nonlinear PID controllers by using direct loop-shaping robust control design approach [24] and equivalent linear parameter-varying control theory [25], respectively. However, those controllers can only compensate for the viscoelasticity of DEAs at a specific frequency. Although Hoffstadt $et.al.$ has developed an adaptive sliding model control method [26] for highly dynamical positioning operations of DEAs up to 200 Hz, it is only verified for very small-signal excitations (amplitude of strain 0.1%) and tracking experiment is not presented. Therefore, high-precision tracking control of DEAs remains elusive because of its complicated viscoelastic behavior.

As discussed above, the main difficulty for such control design lies in the existence of the viscoelastic hysteresis nonlinearity. Although some physical-based models [2], [27] have been proposed to describe the viscoelasticity, they are usually too complicated to design an effective real-time controller. In our recent work on constitutive modelling of DEAs [14], we have investigated the viscoelastic phenomena of DEAs and finally pointed out that the viscoelastic hysteresis loops of DEAs generally match the properties of some phenomenological hysteresis models (such as Prandtl-Ishlinskii model and Preisach model), which is similar to other smart material based actuators (such as piezoelectric actuators) without considering the physical nature. It is well known that phenomenological viscoelastic hysteresis models have been widely used to describe and compensate the viscoelastic hysteresis effect of piezoelectric actuators [28]–[31]. Therefore, inspired from the achievement on control of the piezoelectric actuators, we propose a new control approach for DEAs. To this end, a phenomenological hysteresis model based direct inverse hysteresis compensation (DIHC) approach is firstly constructed to compensate for the hysteresis and then a conventional proportional-integral (PI) feedback controller is developed to mitigate the creep and modeling uncertainty. Finally, sufficient comparative experiments with different sinusoidal trajectories under different frequencies are conducted on a fabricated DEA to verify our development. The experimental results demonstrate that the DIHC controller reduces the maximum tracking error from 40.63% to 6.61%; and the maximum tracking error further decreases down to 3.95% when both the DIHC and PI controllers are employed. To our best knowledge, this work is the first attempt to achieve high-precision tracking control of soft DEAs by combining with a phenomenological-model feedforward compensator and a feedback control law for the viscoelastic compensation.

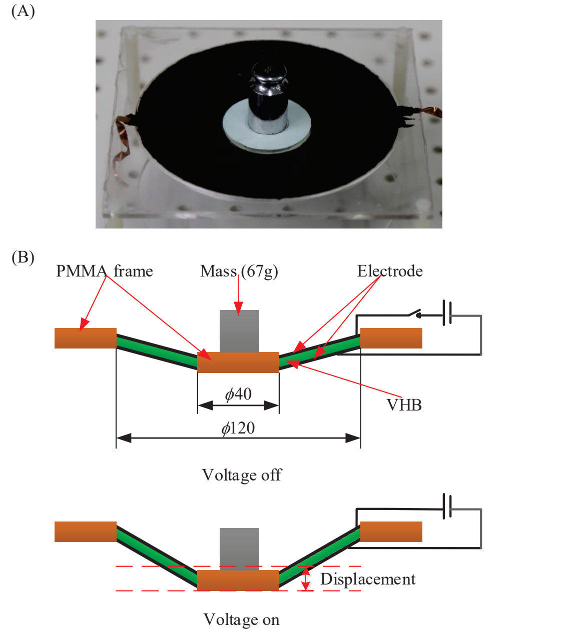

Fig. 2. Description of the conical dielectric elastomer actuator (DEA). (A) A photo of the actual actuator. (B) Working mechanism.

The remainder of this paper is organized as follows. Section II introduces our fabricated conical DEA and experimental platform. In addition, the dynamic response and viscoelasticity of the DEA are characterized in this section. Section III describes the inverse hysteresis compensation approach and Section IV presents the feedback controller. Section V concludes this work.

II. System description

A. Actuator fabrication

A conical DEA shown in Fig. 2A is adopted for proof-of-concept testing. It consists of an equiaxial pre-stretched (pre-stretch ratio 3×3) DE membrane (VHB 4905, undeformed thickness 0.5 mm). A stiff outer frame made by a laser cut acrylic board (thickness 3 mm) is used to support the pre-strain of the DE membrane. Carbon grease (MG Chemical 846-80G) working as compliant electrodes is used to coat both sides of the DE membrane. In order to generate a vertical movement, a mass including of a rigid disk (acrylic board, 17 g) and a weight (50 g) is attached to the center of the DE membrane as an end-effector of the conical DEA. Fig. 2B shows the schematic illustration of the conical DEA's movement when an exciting voltage is applied.

B. Experimental setup

To capture the features of viscoelasticity of the conical DEA and verify the effectiveness of designed controllers, we build an experimental platform as shown in Fig. 3A. The experimental platform is composed of a control module (dSPACE-DS1103 board, dSPACE, Paderborn, Germany), a high voltage

This article has been accepted for publication in a future issue of this journal, but has not been fully edited. Content may change prior to final publication. Citation information: DOI 10.1109/TMECH.2018.2873620, IEEE/ASME Transactions on Mechatronics

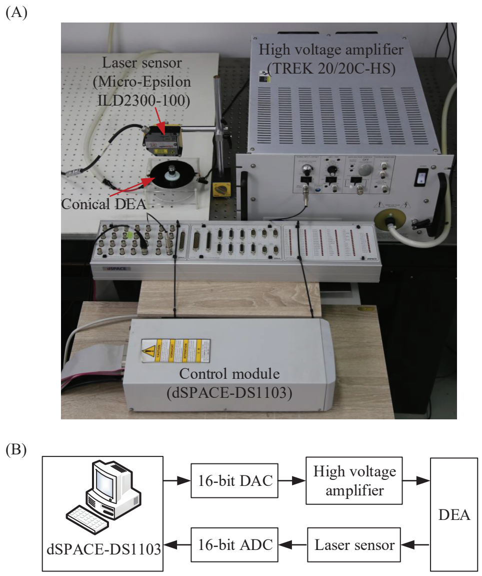

Fig. 3. The experimental platform. (A) Experimental setup. (B) Block diagram.

amplifier (TREK 20/20C-HS, fixed gain of 2000, TREK, New York, USA), a laser sensor (Micro-Epsilon ILD2300-100, range of 100 mm with an analogue output 10 V, Micro-Epsilon, Ortenburg, Germany) and a conical DEA. The control module is used to generate a control signal for the high voltage amplifier and capture the real-time displacement from the laser sensor. The high voltage amplifier can proportionally amplify the control signal and then apply it to the conical DEA. The laser sensor is used to measure the output displacement of the conical DEA. In this work, the sampling time is set to be 1ms. As shown in Fig. 3B, a block diagram of the whole experimental platform is provided. It should be noted that there are several failure phenomena (such as wrinkle and pull-in instability [2]) shall been observed when the amplitude of the exciting voltage exceeds 4 kV. Therefore, we keep the amplitude of the input voltage lower than 3.5 kV. At the meantime, the minimum voltage is 0.5 kV to satisfy the lowest actuated voltage.

C. Experimental phenomena

It is known that the viscoelasticity of the DEA exhibits dynamical behavior. In order to compensate for the viscoelasticity, we should first investigate the dynamical behavior of the DEA. In this sense, a sweep sinusoidal frequency voltage (in the range of 0.01 Hz to 10 Hz) is employed to drive the DEA. Fig. 4 shows the experimental results in the time domain. From the experiment, we can observe that:

i) When the frequency of input voltage is below 1 Hz, the amplitude of the DEA's displacement keeps almost constant and positive. Then, further increasing the frequency, the negative displacement appears. For the convenience of description, we define a critical frequency before the negative displacement appears. In this work, the critical frequency is determined based on the experimental results to be 1 Hz.

ii) When the frequency is in the range of 1 Hz to 4.5 Hz, the response of the DEA becomes complicated. First, the output

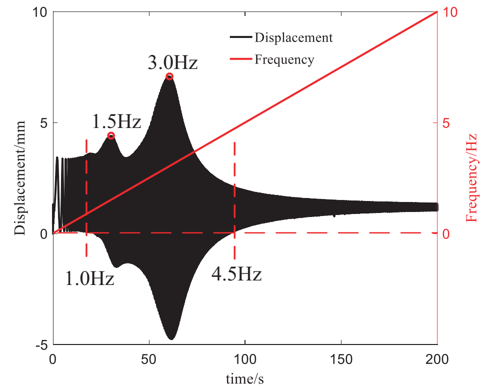

Fig. 4. Experimental results of the sweep frequency test.

displacement contains both positive and negative components, which may be caused by the inertia force of the mass. In addition, we can observe two resonances (1.5 Hz and 3.0 Hz), which have also been reported in [32].

iii) When the frequency exceeds 4.5 Hz, the amplitude rapidly decreases with the increase of frequency.

In this work, as the first attempt to design controllers for viscoelasticity compensation, we restrict the frequency no longer larger than 1 Hz in the following experiments.

Remark: It should be noted that as shown in Fig. 4, the natural frequency of our DEA is about 3.0 Hz. Therefore, in the following development, the maximum input frequency of the voltage on the DEA is limit to 1Hz, avoiding to excite the vibration of the natural frequency.

To further reveal the behaviors of the DEA's viscoelasticity, we conduct several tests with different driven voltages under different amplitudes with different frequencies, which can be expressed as follows:

$$V(t) = \begin{cases} 0.50\sin(2\pi f t - 0.5\pi) + 1.00 & 0 \le t < 1/f \\ 0.75\sin(2\pi f t - 0.5\pi) + 1.25 & 1/f \le t < 2/f \\ 1.00\sin(2\pi f t - 0.5\pi) + 1.50 & 2/f \le t < 3/f \\ 1.25\sin(2\pi f t - 0.5\pi) + 1.75 & 3/f \le t < 4/f \\ 1.50\sin(2\pi f t - 0.5\pi) + 2.00 & 4/f \le t < 5/f \end{cases} \tag{1}$$

where f represents the frequency of the input voltage. In this work, the relations between input voltage and output displacement are measured under different frequencies (in the range of 0.1 Hz to 1 Hz). Fig. 5A shows the input voltage within one cycle when the frequency of the input voltage equals to 0.1 Hz. The output displacement of the conical DEA shown in Fig. 5B demonstrates that it can be explained by two regions: transition region and stable region. As demonstrated in [14] and from the observed responses, during the transition region, the viscoelasticity mainly exhibits the viscoelastic creep effect, while the viscoelastic hysteresis effect of the viscoelasticity is dominated during the stable region. We know that the creep is generally easy for compensation just with traditional feedback control approaches such as the PID controller [16]. However, control of hysteresis effect is more challenging due to its non-smooth nonlinearity [17], [18]. Therefore, at the first step, we mainly focus on the characterization and compensation

This article has been accepted for publication in a future issue of this journal, but has not been fully edited. Content may change prior to final publication. Citation information: DOI 10.1109/TMECH.2018.2873620, IEEE/ASME Transactions on Mechatronics

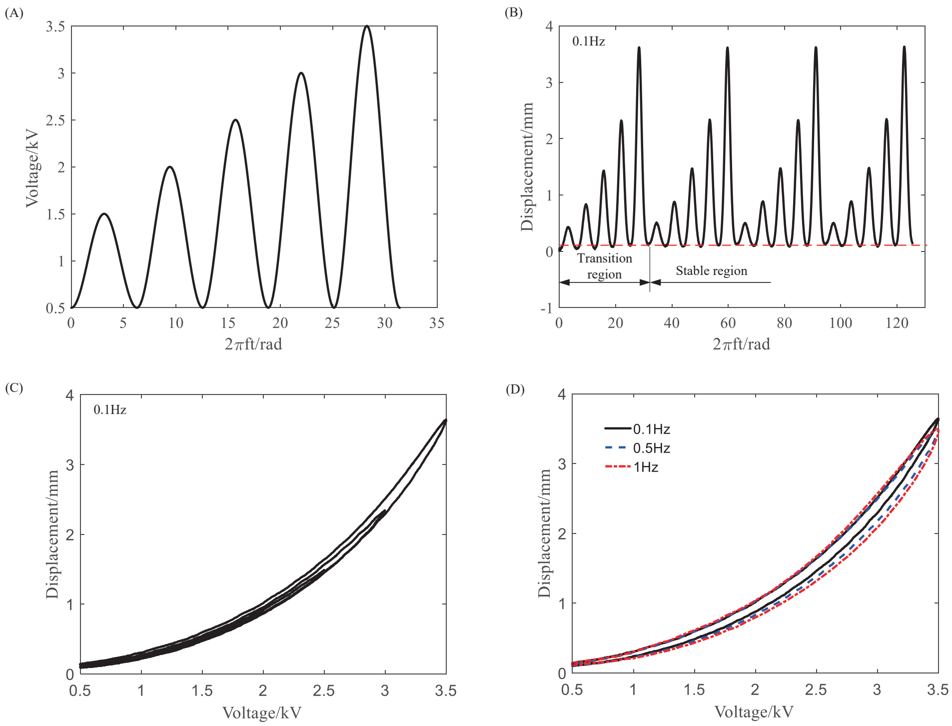

Fig. 5. The response of the conical dielectric elastomer actuator (DEA). (A) The input voltage within one cycle. (B) The output displacement. (C) The hysteresis loop at 0.1 Hz. (D) The comparison of hysteresis loops with different frequencies.

of the hysteresis effect. Then, a feedback controller will be combined for further remedying the creep effect and modeling uncertainty. For the hysteresis description, we first consider the experimental data on the stable region. Fig. 5C shows the hysteresis loops when the frequency of the input voltage equals to 0.1 Hz. The experimental results of hysteresis loops under different frequencies are shown in Fig. 5D. We can see that the hysteresis loops are asymmetric and approximately rate-independent within a frequency range of 0.1 Hz to 1 Hz. It is worth mentioning that the asymmetry of hysteresis loops not only depends on the nonlinear relationship between input voltage and Maxwell stress, but also relies on the viscoelasticity of the conical DEA. Fig. 6 shows that even if the input voltage is linearized, the asymmetry will still exist.

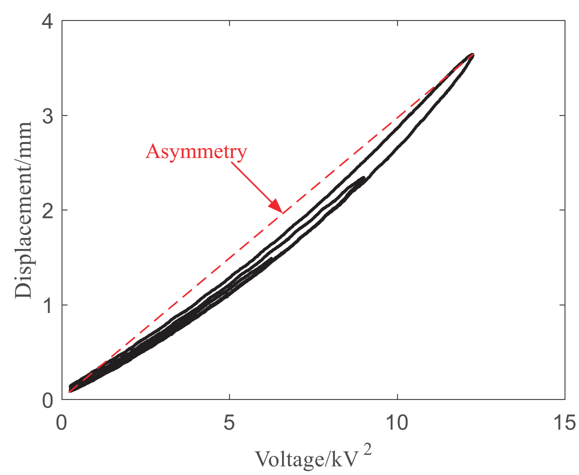

Fig. 6. Illustration of the asymmetric hysteresis loops.

III. Inverse hysteresis compensation

For viscoelastic hysteresis compensation, a phenomenological model is adopted. Considering the fact that the hysteresis loops of the DEA are asymmetric and rate-independent, which are essential for the MPIM in our previous work [31]. Then, the hysteresis can be eliminated by the the DIHC approach, whose flow chart is shown in Fig. 7. For the detailed description on this approach, the reader may refer to [31].

A. Viscoelastic hysteresis description

As shown in Fig. 7, for designing the DIHC controller, the MPIM is directly used to identify the relation of the output displacement and input voltage, which can be expressed as follow [31]:

$$V(t) = g_1 y^3(t) + g_2 y(t) + g_3 + \int_0^R a(r) F_r[y](t)\,dr \quad (2)$$

where g_1, g_2 and g_3 are three constant ratios, $V(t)$ represents the input voltage and $y(t)$ represents the desired output displacement. Besides, $a(r)$ is a density function of $F_r[y](t)$, where $F_r[y](t)$ is a one side play operator expressed as:

$$\begin{aligned} F_r[y](0) &= \max\{y(0) - r, \min\{y(0), 0\}\} \\ F_r[y](t) &= \max\{y(t) - r, \min\{y(t), F_r[y](t-\tau)\}\} \end{aligned} \quad (3)$$

This article has been accepted for publication in a future issue of this journal, but has not been fully edited. Content may change prior to final publication. Citation information: DOI 10.1109/TMECH.2018.2873620, IEEE/ASME Transactions on Mechatronics

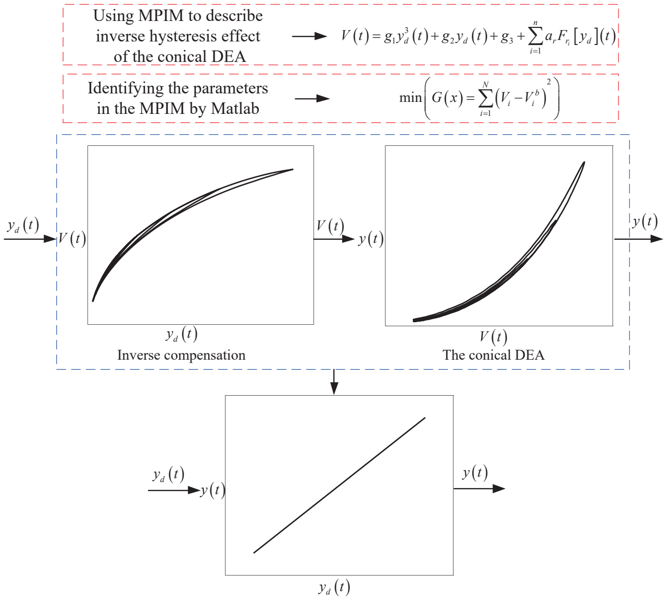

Fig. 7. Flow chart of the DIHC approach.

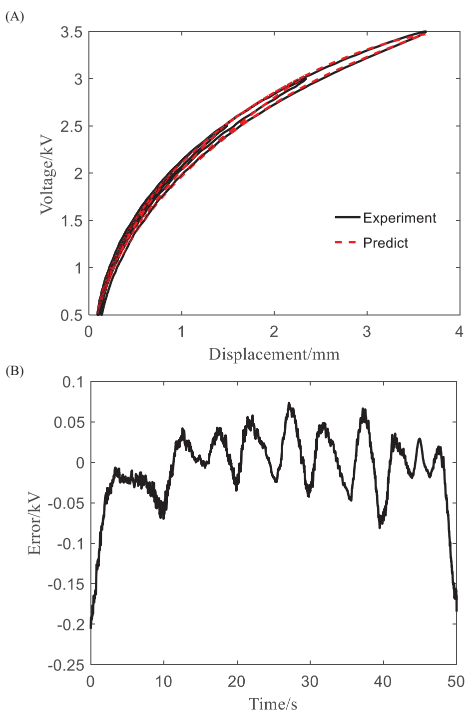

Fig. 8. Identification results. (A) The comparison between experimental data and identified MPIM. (B) Identification Error.

where r is the threshold of the play operator, and τ represents the sampling time. For the convenience of calculation, the digital form of (2) is adopted and it can be written as:

$$V(t) = g_1 y^3(t) + g_2 y(t) + g_3 + \sum_{i=1}^{n} a_r F_{r_i}[y](t) \quad (4)$$

where n represents the number of the adopted play operators for modeling. In this work, five play operators are chosen and a MATLAB function $lsqnonlin$ (a nonlinear least squares

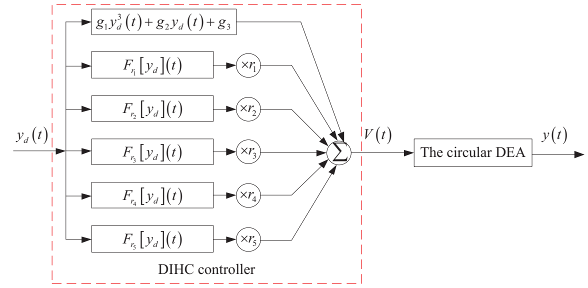

Fig. 9. Block diagram of the DIHC controller law.

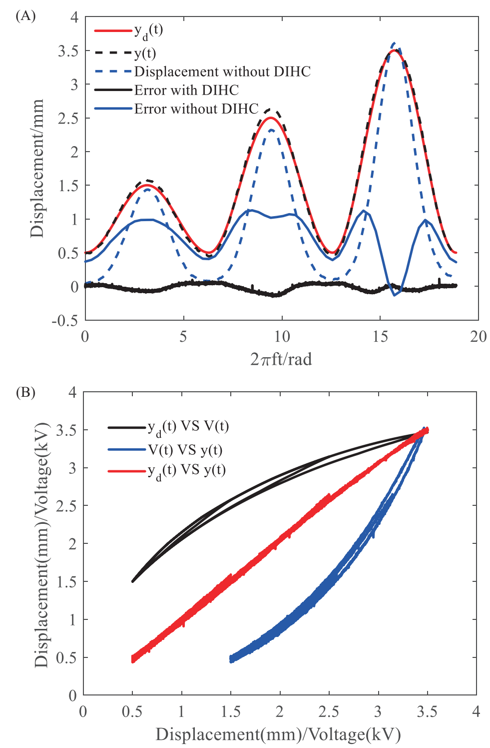

Fig. 10. Feedforward experiment results with the DIHC controller. (A) Comparison between reference displacement $y_d(t)$ and actual displacement $y(t)$. (B) Three kinds of relationships between input and output, including reference displacement $y_d(t)$ vs control voltage $V(t)$, control voltage $V(t)$ vs actual displacement $y(t)$, reference displacement $y_d(t)$ vs actual displacement $y(t)$.

algorithm) is adopted to identify the parameters of the MPIM. To employ this algorithm, the objective function is selected as:

$$F = \min \sum (V - V_{MPIM})^2 \quad (5)$$

where V and V_{MPIM} represent the experimental data and predicted result, respectively. The initial value of each parameter

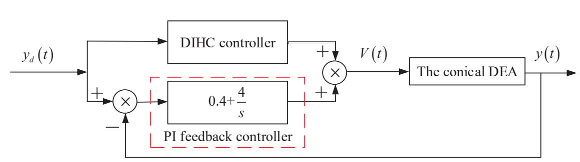

Fig. 11. Block diagram of the proposed two-level tracking control approach for the DEA.

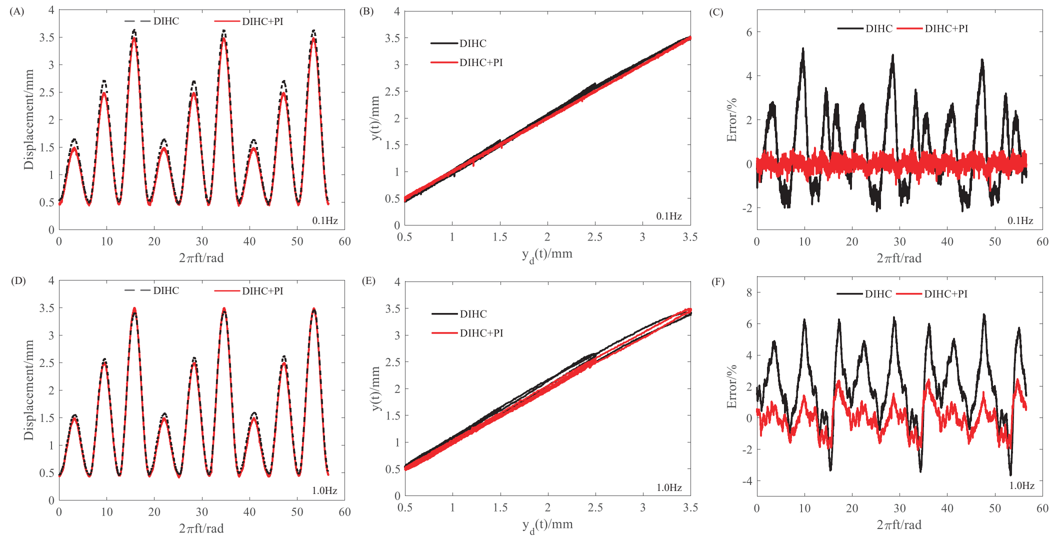

Fig. 12. Experimental results with both DIHC and PI feedback controllers under different frequencies. When the frequency of the input voltage is 0.1Hz: (A) the real time output displacements; (B) the relationships between reference displacement and actual displacement; (C) the comparison of tracking errors. When the frequency increases to 1Hz: (D) the real time output displacements; (E) the relationships between reference displacement and actual displacement; (F) the comparison of tracking errors.

is randomly generated by a MATLB function $rand$. The low limit and upper limit values of all parameters are -3 and 3, respectively. The maximum iteration is set to be 1000.

Table I lists the identified parameters of the MPIM when the input and output are in normalized cases. Fig. 8A shows the comparison of the experiment results and identified model predictions. We can see from Fig. 8B that the MPIM can precisely describe the viscoelastic hysteresis effect of the tested DEA.

TABLE I
PARAMETERS OF THE IDENTIFIED MPIM

i	r_i	a_i	g_i
1	0	-0.7243	-0.2657
2	0.1	-0.1067	2.1901
3	0.2	-0.1150	0.0012
4	0.4	-0.0415	
5	0.9	-0.0435	

B. *DIHC controller design*

Based on the identified MPIM, a DIHC controller is designed to compensate for the hysteresis effect of the conical DEA. Fig. 9 shows the block diagram of the control law. To verify the effectiveness of the controller, different sinusoidal trajectory tracking experiments are conducted. For the convenience of tracking performance description, we define two tracking errors, in terms of the root-mean-square error e_{rms} and the maximum tracking error e_m.

$$e_{rms} = \frac{\sqrt{\frac{1}{N}\sum\limits_{i=1}^{N}\left(y_{di}-y_i\right)^2}}{\max(y_{di})-\min(y_{di})} \times 100\% \tag{6}$$

$$e_m = \frac{\max(y_{di}-y_i)}{\max(y_{di})-\min(y_{di})} \times 100\% \tag{7}$$

where y_i and y_{di} represent the actual displacement and reference displacement, respectively. N is the sampling quantity within one cycle. The experimental results are shown in Fig. 10A, which clearly demonstrate that with the DIHC controller, e_{rms} and e_m are 1.73% and 4.75%, respectively. However, if the DIHC controller is not applied, e_{rms} and e_m will reach 27.04% and 38.14%, respectively. Therefore, the DIHC controller is effective for viscoelastic hysteresis compensation.

To further illustrate the compensation effectiveness, Fig. 10B summarizes three relation curves, including reference displacement $y_d\left(t\right)$ vs control voltage $V\left(t\right)$, control voltage $V\left(t\right)$ vs actual displacement $y\left(t\right)$, and reference displacement $y_d\left(t\right)$ vs actual displacement $y\left(t\right)$. It can be seen that the DIHC controller generates inverse hysteresis loops (black line) to compensate for the hysteresis loops (blue line), such that the relation between reference displacement and actual displacement can be approximately linearized (red line). Of course, due to the model uncertainty and creep effect, the actual displacement cannot completely follow the reference trajectory. To further improve tracking precision, the following feedback controller shall be developed.

IV. Feedback controller design

Combining with the feedforward DIHC controller, a PI feedback controller is further designed to remedy the model uncertainty and creep effect of the DEA. The control block is shown in Fig. 11. We may mention that the parameters of the PI feedback controller are selected based on prior experiments and trial and error method. In this work, the transfer function of the PI feedback controller is expressed as:

$$PI = 0.4 + \frac{4}{s} \tag{8}$$

To verify the effectiveness of the two-level tracking controller, several experiments are conducted with different sinusoidal trajectories with different amplitudes and frequencies.

This article has been accepted for publication in a future issue of this journal, but has not been fully edited. Content may change prior to final publication. Citation information: DOI 10.1109/TMECH.2018.2873620, IEEE/ASME Transactions on Mechatronics

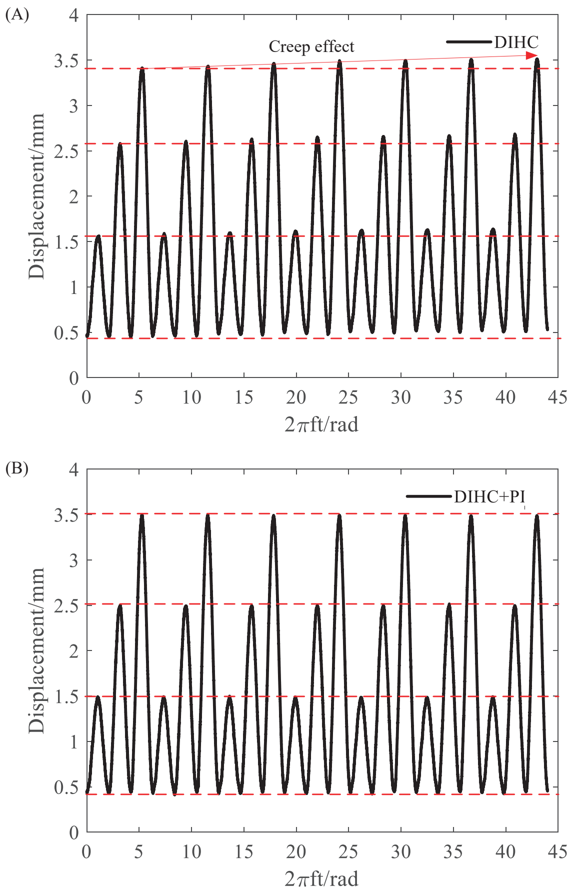

Fig. 13. The experimental results of the creep compensation when the frequency of the input voltage is 1Hz. (A) The DIHC controller cannot remove the creep effect of the output displacement. (B) When a PI feedback controller is further employed, the creep effect is completely estimated.

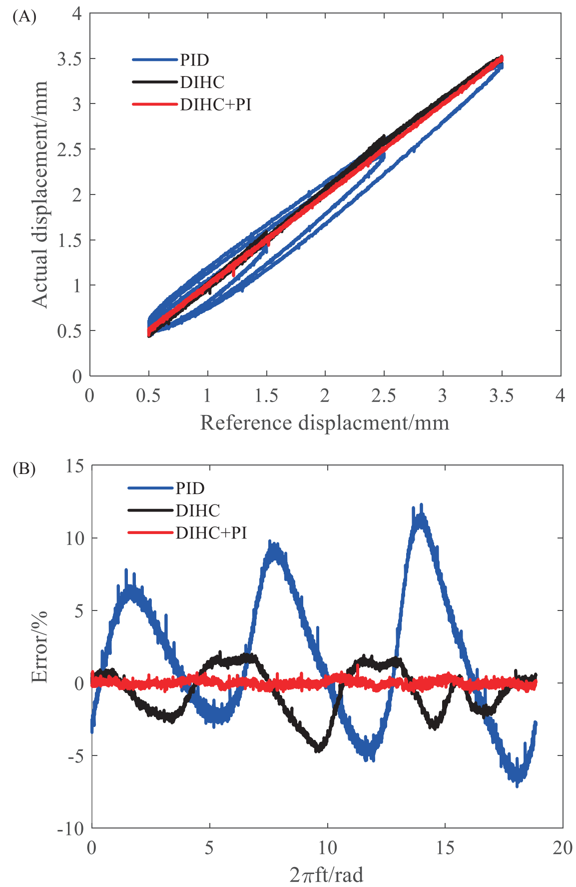

Fig. 14. Comparisons between different control strategies. (A) The relationships between reference displacement and actual displacement. (B) The comparison of tracking errors.

Fig. 12 shows two examples of the tracking results with both DIHC and PI feedback controllers. It can be seen that: i) When the input frequency equals to 0.1Hz (Fig. 12A-C), e_{rms} and e_m are 0.19% and 1.24%, respectively. Comparing with purely DIHC controller, e_{rms} and e_m are reduced by 89.01% and 73.89%, respectively. ii) When the input frequency increases to 1Hz (Fig. 12D-F), e_{rms} and e_m decrease from 2.93% to 0.92% and 6.61% to 2.48%, respectively. Further experiments are listed in Table II, it clearly demonstrates that our tracking control approach can work well within the frequency range of 0.1 Hz to 1 Hz. In addition, Fig. 13 shows that the DIHC controller cannot remove the viscoelastic creep effect, but the PI feedback controller can.

To further elucidate the role of the DIHC controller in our tracking control approach, we conduct a tracking test when only the PI feedback controller is applied. The experiment results are shown in Fig. 14. We can see that the maximum tracking error is more than 12% and hysteresis effect still exists. However, the drift phenomenon due to creep effect has been removed. Therefore, we can note that the PI feedback controller is effective for creep compensation, but not for hysteresis compensation.

TABLE II
TRACKING ERRORS UNDER DIFFERENT FREQUENCIES

Controller	Without		DIHC		DIHC+PI	
Frequency/Hz	$e_{rms}/\%$	$e_m/\%$	$e_{rms}/\%$	$e_m/\%$	$e_{rms}/\%$	$e_m/\%$
0.1	27.04	38.14	1.73	4.75	0.19	1.24
0.2	27.38	38.50	1.53	4.34	0.37	1.36
0.3	27.63	38.79	1.59	4.41	0.74	1.81
0.4	27.19	38.71	1.85	4.95	1.16	2.53
0.5	27.52	39.25	1.98	5.07	1.38	3.02
0.6	27.33	39.56	1.94	5.03	1.33	2.98
0.7	27.55	39.79	1.98	5.06	1.64	3.65
0.8	28.38	40.40	1.86	4.71	1.86	3.86
0.9	27.36	40.47	1.95	4.85	1.80	3.95
1.0	27.52	40.63	2.93	6.61	0.92	2.48

V. Conclusion

In this work, we focus on achieving high precision tracking control of a conical DEA with the viscoelastic compensation. To this end, we investigate the viscoelastic response of the DEA. The experimental results show that when the frequency of input is lower than a critical frequency, the viscoelasticity presents two main features: i) there is creep effect of the output displacement, which generally lasts during the first few cycles. ii) The hysteresis loops are asymmetric and rate-independent, which are dominating after the first few cycles. To remedy the viscoelasticity in terms of creep and hysteresis nonlinearities, we first present a DIHC controller for the hysteresis description and compensation and then a conventional PI feedback controller is combined to compensate for the model uncertainty and creep effect. Finally, tests on tracking different sinusoidal trajectories with the frequencies of 0.1 Hz to 1 Hz are conducted. Comparative experimental results clearly demonstrate the effectiveness of the developed controllers for high-precision trajectory tracking.

REFERENCES

[1] Ailish OHalloran, Fergal OMalley, and Peter McHugh. A review on dielectric elastomer actuators, technology, applications, and challenges. *Journal of Applied Physics*, 104(7):071101, 2008.

[2] G. Y. Gu, J. Zhu, L. M. Zhu, and X. Y. Zhu. A survey on dielectric elastomer actuators for soft robots. *Bioinspiration and Biomimetics*, 12(1):011003, 2017.

[3] Guggi Kofod and Roy Kornbluh. *Chapter 16: Dielectric Elastomer Actuators as Intelligent Materials for Actuation, Sensing and Generation*, pages 396–423. The Royal Society of Chemistry, 2008.

[4] R. Pelrine, R. Kornbluh, Q. B. Pei, and J. Joseph. High-speed electrically actuated elastomers with strain greater than 100%. *Science*, 287(5454):836–839, 2000.

[5] Christoph Keplinger, Jeong-Yun Sun, Choon Chiang Foo, Philipp Rothemund, George M. Whitesides, and Zhigang Suo. Stretchable, Transparent, Ionic Conductors. *Science*, 341(6149):984–987, 2013.

[6] F. Carpi, C. Salaris, and D. De Rossi. Folded dielectric elastomer actuators. *Smart Materials and Structures*, 16(2):S300–S305, 2007.

[7] Farah Afiqa Mohd Ghazali, Che Ken Mah, Alaa AbuZaiter, Pei Song Chee, and Mohamed Sultan Mohamed Ali. Soft dielectric elastomer actuator micropump. *Sensors and Actuators A: Physical*, 263:276–284, 2017.

[8] A. Girard, J. P. L. Bigue, B. M. O'Brien, T. A. Gisby, I. A. Anderson, and J. S. Plante. Soft Two-Degree-of-Freedom Dielectric Elastomer Position Sensor Exhibiting Linear Behavior. *IEEE/ASME Transactions on Mechatronics*, 20(1):105–114, 2015.

[9] Jun Shintake, Samuel Rosset, Bryan Schubert, Dario Floreano, and Herbert Shea. Versatile soft grippers with intrinsic electroadhesion based on multifunctional polymer actuators. *Advanced Materials*, 28(2):231–238, 2016.

[10] F. F. Chen and M. Y. Wang. Simulation of networked dielectric elastomer balloon actuators. *IEEE Robotics and Automation Letters*, 1(1):221–226, 2016.

[11] F. F. Chen, M. Y. Wang, J. Zhu, and Y. F. Zhang. Interactions between dielectric elastomer actuators and soft bodies. *Soft Robotics*, 3(4):161–169, 2016.

[12] Tiefeng Li, Guorui Li, Yiming Liang, Tingyu Cheng, Jing Dai, Xuxu Yang, Bangyuan Liu, Zedong Zeng, Zhilong Huang, and Yingwu Luo. Fast-moving soft electronic fish. *Science Advances*, 3(4):e1602045, 2017.

[13] Canh Toan Nguyen, Hoa Phung, Tien Dat Nguyen, Hosang Jung, and Hyouk Ryeol Choi. Multiple-Degrees-of-Freedom Dielectric Elastomer Actuators for Soft Printable Hexapod Robot. *Sensors and Actuators A: Physical*, 267:505–516, 2017.

[14] G. Y. Gu, U Gupta, J. Zhu, L. M. Zhu, and X. Y. Zhu. Modeling of viscoelastic electromechanical behavior in a soft dielectric elastomer actuator. *IEEE Transactions on Robotics*, 33(5):1263–1271, 2017.

[15] J. Zou, G. Y. Gu, and L. M. Zhu. Open-loop control of creep and vibration in dielectric elastomer actuators with phenomenological models. *IEEE/ASME Transactions on Mechatronics*, 22(1):51–58, 2017.

[16] R. Zhang, P. Iravani, and P. Keogh. Closed loop control of force operation in a novel self-sensing dielectric elastomer actuator. *Sensors and Actuators A: Physical*, 264:123–132, 2017.

[17] Isaak D Mayergoyz. *Mathematical models of hysteresis and their applications*. Academic Press, 2003.

[18] Martin Brokate and Jrgen Sprekels. *Hysteresis and phase transitions*, volume 121. Springer-Verlag, New York, 1996.

[19] G. Y. Gu, L. M. Zhu, C. Y. Su, H. Ding, and S. Fatikow. Modeling and Control of Piezo-Actuated Nanopositioning Stages: A Survey. *IEEE Transactions on Automation Science and Engineering*, 13(1):313–332, 2016.

[20] F Branz and A Francesconi. Modelling and control of double-cone dielectric elastomer actuator. *Smart Materials and Structures*, 25(9):095040, 2016.

[21] N. H. Chuc, N. H. L. Vuong, D. S. Kim, H. P. Moon, J. C. Koo, Y. K. Lee, J. D. Nam, and H. R. Choi. Fabrication and Control of Rectilinear Artificial Muscle Actuator. *IEEE/ASME Transactions on Mechatronics*, 16(1):167–176, 2011.

[22] Rosset Samuel, M. OBrien Benjamin, Gisby Todd, Xu Daniel, R. Shea Herbert, and A. Anderson Iain. Self-sensing dielectric elastomer actuators in closed-loop operation. *Smart Materials and Structures*, 22(10):104018, 2013.

[23] Todd A. Gisby, Benjamin M. O'Brien, Sheng Q. Xie, Emilio P. Calius, and Iain A. Anderson. Closed loop control of dielectric elastomer actuators. In *SPIE Smart Structures and Materials + Nondestructive Evaluation and Health Monitoring*, volume 7976, page 797920. SPIE, 2011.

[24] G. Rizzello, D. Naso, A. York, and S. Seelecke. Modeling, Identification, and Control of a Dielectric Electro-Active Polymer Positioning System. *IEEE Transactions on Control Systems Technology*, 23(2):632–643, 2015.

[25] Gianluca Rizzello, David Naso, Biagio Turchiano, and Stefan Seelecke. Robust Position Control of Dielectric Elastomer Actuators Based on LMI Optimization. *IEEE Transactions on Control Systems Technology*, 24(6):1909–1921, 2016.

[26] T. Hoffstadt and J. Maas. Adaptive Sliding Model Position Control for Dielectric Elastomer Actuators. *IEEE/ASME Transactions on Mechatronics*, 22(5):2241–2251, 2017.

[27] Z. Suo. Theory of dielectric elastomers. *Acta Mechanica Solida Sinica*, 23(6):549–578, 2010.

[28] Q. Q. Wang and C. Y. Su. Robust adaptive control of a class of nonlinear systems including actuator hysteresis with PrandtlcIshlinskii presentations. *Automatica*, 42(5):859–867, 2006.

[29] M. Al Janaideh, S. Rakheja, and C. Y. Su. An Analytical Generalized Prandtl-Ishlinskii Model Inversion for Hysteresis Compensation in Micropositioning Control. *IEEE/ASME Transactions on Mechatronics*, 16(4):734–744, 2011.

[30] Z. Li and J. Shan. Modeling and Inverse Compensation for Coupled Hysteresis in Piezo-Actuated Fabry-Perot Spectrometer. *IEEE/ASME Transactions on Mechatronics*, 22(4):1903–1913, 2017.

[31] G. Y. Gu and L. M. Zhu. Motion control of piezoceramic actuators with creep, hysteresis and vibration compensation. *Sensors and Actuators A: Physical*, 197:76–87, 2013.

[32] G Rizzello, M Hodgins, D Naso, A York, and S Seelecke. Modeling of the effects of the electrical dynamics on the electromechanical response of a DEAP circular actuator with a masscspring load. *Smart Materials and Structures*, 24(9):094003, 2015.

Guoying Gu (S'10-M'13) received the B.E. degree (with honors) in electronic science and technology, and the Ph.D. degree (with honors) in mechatronic engineering from Shanghai Jiao Tong University, Shanghai, China, in 2006 and 2012, respectively.

Supported by the Alexander von Humboldt Foundation, he was as a Humboldt Postdoc Fellow at University of Oldenburg, Oldenburg, Germany. He was a Visiting Scholar at Massachusetts Institute of Technology, USA, National University of Singapore, Singapore and Concordia University, Canada. Since October 2012, Dr. Gu has worked at Shanghai Jiao Tong University, where he is currently appointed as a Professor of School of Mechanical Engineering. His research interests include soft robotics, bioinspired robot design and motion control, smart materials actuators and sensors, and additive manufacturing with soft materials. He is the author or co-author of over 70 publications, which have appeared in journals, as book chapters and in conference proceedings.

Dr. Gu is the winner of multiple wards including Young Changjiang Scholar of the Ministry of Education, National Science Fund for Excellent Young Scholars, The first prize of natural science of Ministry of Education, Best Paper Award at the 2016 International Conference on Intelligent Robotics and Applications and 2011 IEEE International Conference on Information and Automation. He is a member of the IEEE and ASME. Now he serves as Associate Editor of International Journal of Advanced Robotic Systems. He has also served for several international conferences/symposiums as Chair, Associate Editor or Program Committee Member.

This article has been accepted for publication in a future issue of this journal, but has not been fully edited. Content may change prior to final publication. Citation information: DOI 10.1109/TMECH.2018.2873620, IEEE/ASME Transactions on Mechatronics

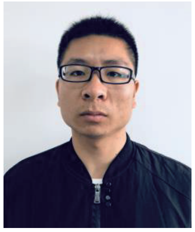

Jiang Zou received the B.E. degree (with honors) in mechanical engineering from University of Science and Technology Beijing, Beijing, China, in 2014, and he is currently working toward the Ph.D. degree in Shanghai Jiao Tong University. His research interests include design, modeling and control of soft robotics.